*

*

Renormalised vacuum polarisation on topological black holes

Thomas Morley

School of Mathematics and Statistics
University of Sheffield

tmmorley1@sheffield.ac.uk

YTF 11, 20 December 2018

In collaboration with Elizabeth Winstanley (UOS) and Peter Taylor (DCU)

Overview

Schwarzschild anti-de Sitter spacetime

Schwarzschild anti-de Sitter (SadS) spacetime is a solution of Einstein's equations with a negative cosmological constant.

Schwarzschild anti-de Sitter spacetime

Schwarzschild anti-de Sitter (SadS) spacetime is a solution of Einstein's equations with a negative cosmological constant.

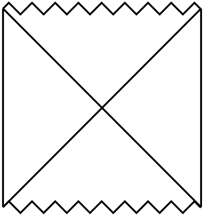

Schwarzschild anti-de Sitter spacetime

Schwarzschild anti-de Sitter (SadS) spacetime is a solution of Einstein's equations with a negative cosmological constant.

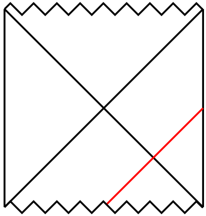

Schwarzschild anti-de Sitter spacetime

Schwarzschild anti-de Sitter (SadS) spacetime is a solution of Einstein's equations with a negative cosmological constant.

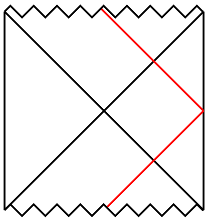

Schwarzschild anti-de Sitter spacetime

Schwarzschild anti-de Sitter (SadS) spacetime is a solution of Einstein's equations with a negative cosmological constant.

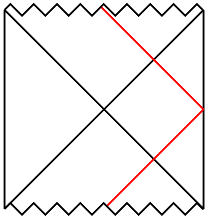

Why adS space?

Line element

$$ds^2 = -f(r)dt^2 + f(r)^{-1}dr^2 + r^2 d\Omega_k^2$$

Line element

$$ds^2 = -f(r)dt^2 + f(r)^{-1}dr^2 + r^2 d\Omega_k^2$$

$$f(r) = k - \frac{2M}{r} + \frac{r^2}{L^2}.$$

Line element

$$ds^2 = -f(r)dt^2 + f(r)^{-1}dr^2 + r^2 d\Omega_k^2$$

$$f(r) = k - \frac{2M}{r} + \frac{r^2}{L^2}.$$

The cosmological constant $\Lambda = -3L^{-2}$, with L the curvature lengthscale.

Line element

$$ds^2 = -f(r)dt^2 + f(r)^{-1}dr^2 + r^2 d\Omega_k^2$$

$$f(r) = k - \frac{2M}{r} + \frac{r^2}{L^2}.$$

The cosmological constant $\Lambda = -3L^{-2}$, with L the curvature lengthscale.

The parameter k can take the values $+1, 0$ or -1.

Topological black holes [1]

$$d\Omega_k^2 = \begin{cases} d\theta^2 + \sin^2\theta d\varphi^2, & k = 1 \\ d\theta^2 + \theta^2 d\varphi^2, & k = 0 \\ d\theta^2 + \sinh^2\theta d\varphi^2, & k = -1 \end{cases}$$

[1] D. Birmingham, *CQG*, 1999

Topological black holes [1]

$$d\Omega_k^2 = \begin{cases} d\theta^2 + \sin^2\theta d\varphi^2, & k = 1 \\ d\theta^2 + \theta^2 d\varphi^2, & k = 0 \\ d\theta^2 + \sinh^2\theta d\varphi^2, & k = -1 \end{cases}$$

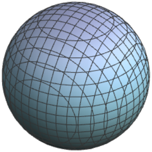

[1] D. Birmingham, *CQG*, 1999

Topological black holes [1]

$$d\Omega_k^2 = \begin{cases} d\theta^2 + \sin^2\theta d\varphi^2, & k=1 \\ d\theta^2 + \theta^2 d\varphi^2, & k=0 \\ d\theta^2 + \sinh^2\theta d\varphi^2, & k=-1 \end{cases}$$

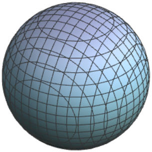

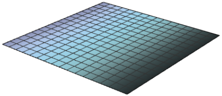

[1] D. Birmingham, *CQG*, 1999

Topological black holes [1]

$$d\Omega_k^2 = \begin{cases} d\theta^2 + \sin^2\theta d\varphi^2, & k = 1 \\ d\theta^2 + \theta^2 d\varphi^2, & k = 0 \\ d\theta^2 + \sinh^2\theta d\varphi^2, & k = -1 \end{cases}$$

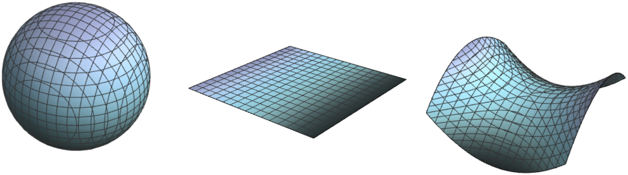

[1] D. Birmingham, *CQG*, 1999

Quantum Field Theory

$$G_{\mu\nu} + \Lambda g_{\mu\nu} = 8\pi T_{\mu\nu}$$

Quantum Field Theory

$$G_{\mu\nu} + \Lambda g_{\mu\nu} = 8\pi \langle \hat{T}_{\mu\nu} \rangle$$

Quantum Field Theory

$$G_{\mu\nu} + \Lambda g_{\mu\nu} = 8\pi \langle \hat{T}_{\mu\nu} \rangle$$

The vacuum polarisation

$$\langle 0 | \hat{\phi}^2 | 0 \rangle = \langle \hat{\phi}^2 \rangle$$

Quantum Field Theory

$$G_{\mu\nu} + \Lambda g_{\mu\nu} = 8\pi \langle \hat{T}_{\mu\nu} \rangle$$

The vacuum polarisation

$$\langle 0 | \hat{\phi}^2 | 0 \rangle = \langle \hat{\phi}^2 \rangle$$

ϕ is a massless, conformally coupled scalar field

$$\left(\Box - \frac{1}{6} R \right) \phi = 0$$

Quantum Field Theory

$$G_{\mu\nu} + \Lambda g_{\mu\nu} = 8\pi \langle \hat{T}_{\mu\nu} \rangle$$

The vacuum polarisation

$$\langle 0 | \hat{\phi}^2 | 0 \rangle = \langle \hat{\phi}^2 \rangle$$

ϕ is a massless, conformally coupled scalar field

$$\left(\Box - \frac{1}{6} R \right) \phi = 0$$

Boundary conditions: $\phi = 0$ (Dirichlet) or $\nabla \phi = 0$ (Neumann)

Vacuum Polarisation

In the absence of an external field, virtual particles are created and annihilated in the vacuum state.

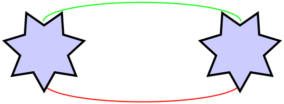

Vacuum Polarisation

In the absence of an external field, virtual particles are created and annihilated in the vacuum state.

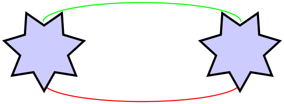

When a black hole is present, one of the particles can be trapped behind the event horizon, whilst the other escapes.[2]

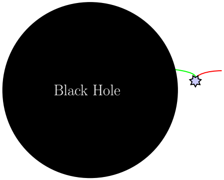

[2]S. W. Hawking, *Communications in math. phys.*, 1975

Vacuum Polarisation

Measures difference between VEVs of observables in the gravitational field and VEVs when there is no gravitational field.

Vacuum Polarisation

Measures difference between VEVs of observables in the gravitational field and VEVs when there is no gravitational field.

We have Euclideanised $t \rightarrow i\tau$

Vacuum Polarisation

Measures difference between VEVs of observables in the gravitational field and VEVs when there is no gravitational field.

We have Euclideanised $t \rightarrow i\tau$

$$\langle \phi^2 \rangle = \lim_{x' \rightarrow x} G_E(x, x')$$

The Euclidean Green's function

In SadS, the Euclidean Green's function satisfies

$$\left(\Box - \frac{1}{6}R\right) G_E(\tau, r, \theta, \varphi;\, \tau', r', \theta', \varphi') = -\frac{1}{r^2}\delta(\tau - \tau')\delta(r - r')\delta(\Omega_k, \Omega_k')$$

The Euclidean Green's function

In SadS, the Euclidean Green's function satisfies

$$\left(\Box - \frac{1}{6}R\right) G_E(\tau, r, \theta, \varphi;\, \tau', r', \theta', \varphi') = -\frac{1}{r^2}\delta(\tau-\tau')\delta(r-r')\delta(\Omega_k, \Omega'_k)$$

$$\delta(\Omega_k, \Omega'_k) = \begin{cases} \frac{1}{\sin\theta}\delta(\theta-\theta')\delta(\varphi-\varphi'), & k=1 \\ \frac{1}{\theta}\delta(\theta-\theta')\delta(\varphi-\varphi'), & k=0 \\ \frac{1}{\sinh\theta}\delta(\theta-\theta')\delta(\varphi-\varphi'), & k=-1. \end{cases}$$

The Euclidean Green's function

We find

$$G_E(x,x')_{k=1} = \frac{\kappa}{2\pi}\sum_{n=-\infty}^{\infty} e^{in\kappa\Delta\tau}\sum_{\ell=0}^{\infty}\frac{2\ell+1}{4\pi}P_\ell(\cos\gamma_S)g_{n\ell}(r;r')$$

The Euclidean Green's function

We find

$$G_E(x,x')_{k=1} = \frac{\kappa}{2\pi}\sum_{n=-\infty}^{\infty} e^{in\kappa\Delta\tau}\sum_{\ell=0}^{\infty}\frac{2\ell+1}{4\pi}P_\ell(\cos\gamma_S)g_{n\ell}(r;r')$$

$$G_E(x,x')_{k=0} = \frac{\kappa}{2\pi}\sum_{n=-\infty}^{\infty} e^{in\kappa\Delta\tau}\int_0^\infty \frac{\alpha}{2\pi}J_0(\alpha\gamma_R)g_{n\alpha}(r;r')d\alpha$$

The Euclidean Green's function

We find

$$G_E(x,x')_{k=1} = \frac{\kappa}{2\pi}\sum_{n=-\infty}^{\infty} e^{in\kappa\Delta\tau}\sum_{\ell=0}^{\infty}\frac{2\ell+1}{4\pi}P_\ell(\cos\gamma_S)g_{n\ell}(r;r')$$

$$G_E(x,x')_{k=0} = \frac{\kappa}{2\pi}\sum_{n=-\infty}^{\infty} e^{in\kappa\Delta\tau}\int_0^\infty \frac{\alpha}{2\pi}J_0(\alpha\gamma_R)g_{n\alpha}(r;r')d\alpha$$

$$G_E(x,x')_{k=-1} = \frac{\kappa}{2\pi}\sum_{n=-\infty}^{\infty} e^{in\kappa\Delta\tau}\int_0^\infty \frac{\rho}{2\pi}\tanh\rho\; P_{-\frac{1}{2}+i\rho}(\cosh\gamma_H) \times g_{n\rho}(r;r')d\rho$$

This diverges in the coincidence limit $x' \to x$.

Renormalisation[3]

All divergences are encapsulated in the Hadamard parametrix

$$G_{Had}(x,x') = \frac{1}{8\pi^2}\frac{\Delta^{1/2}(x,x')}{\sigma(x,x')}.$$

[3] P. Taylor, C. Breen, *Phys. Rev. D, APS*, 2017

Renormalisation[3]

All divergences are encapsulated in the Hadamard parametrix

$$G_{Had}(x, x') = \frac{1}{8\pi^2} \frac{\Delta^{1/2}(x, x')}{\sigma(x, x')}.$$

We renormalise by performing the subtraction

$$\langle \phi^2 \rangle_{ren} = \lim_{x' \to x} \{ G_E(x, x') - G_{Had}(x, x') \}.$$

[3] P. Taylor, C. Breen, *Phys. Rev. D, APS*, 2017

Renormalisation[3]

All divergences are encapsulated in the Hadamard parametrix

$$G_{Had}(x,x') = \frac{1}{8\pi^2}\frac{\Delta^{1/2}(x,x')}{\sigma(x,x')}.$$

We renormalise by performing the subtraction

$$\langle\phi^2\rangle_{ren} = \lim_{x'\to x}\{G_E(x,x') - G_{Had}(x,x')\}.$$

But taking a divergent term away from another divergent term is not easy!

[3] P. Taylor, C. Breen, *Phys. Rev. D, APS*, 2017

The Extended Coordinates method

We write G_{Had} as a mode-sum that matches the form of G_E:

$$G_{Had}(x,x')_{k=1} = \frac{1}{8\pi^2}\sum_{n=-\infty}^{\infty} e^{in\kappa\Delta\tau}\sum_{\ell=0}^{\infty}(2\ell+1)P_\ell(\cos\gamma_S)\sum_{i=0}^{2}\sum_{j=-i}^{i}\Psi_{n\ell}(i,j|r)$$

The Extended Coordinates method

We write G_{Had} as a mode-sum that matches the form of G_E:

$$G_{Had}(x,x')_{k=1} = \frac{1}{8\pi^2}\sum_{n=-\infty}^{\infty} e^{in\kappa\Delta\tau}\sum_{\ell=0}^{\infty}(2\ell+1)P_\ell(\cos\gamma_S)\sum_{i=0}^{2}\sum_{j=-i}^{i}\Psi_{n\ell}(i,j|r)$$

$$G_{Had}(x,x')_{k=0} = \frac{1}{8\pi^2}\sum_{n=-\infty}^{\infty} e^{in\kappa\Delta\tau}\int_0^\infty \alpha J_0(\alpha\gamma_R)\sum_{i=0}^{2}\sum_{j=-i}^{i}\Psi_{n\alpha}(i,j|r)d\alpha$$

The Extended Coordinates method

We write G_{Had} as a mode-sum that matches the form of G_E:

$$G_{Had}(x,x')_{k=1} = \frac{1}{8\pi^2}\sum_{n=-\infty}^{\infty} e^{in\kappa\Delta\tau}\sum_{\ell=0}^{\infty}(2\ell+1)P_\ell(\cos\gamma_S)\sum_{i=0}^{2}\sum_{j=-i}^{i}\Psi_{n\ell}(i,j|r)$$

$$G_{Had}(x,x')_{k=0} = \frac{1}{8\pi^2}\sum_{n=-\infty}^{\infty} e^{in\kappa\Delta\tau}\int_0^\infty \alpha J_0(\alpha\gamma_R)\sum_{i=0}^{2}\sum_{j=-i}^{i}\Psi_{n\alpha}(i,j|r)d\alpha$$

$$G_{Had}(x,x')_{k=-1} = \frac{1}{8\pi^2}\sum_{n=-\infty}^{\infty} e^{in\kappa\Delta\tau}\int_0^\infty \rho\tanh(\rho\pi)P_{-\frac{1}{2}+i\rho}(\cosh\gamma_H) \times\sum_{i=0}^{2}\sum_{j=-i}^{i}\Psi_{n\rho}(i,j|r)d\rho$$

The Extended Coordinates method

We write G_{Had} as a mode-sum that matches the form of G_E:

$$G_{Had}(x,x')_{k=1} = \frac{1}{8\pi^2}\sum_{n=-\infty}^{\infty} e^{in\kappa\Delta\tau}\sum_{\ell=0}^{\infty}(2\ell+1)P_\ell(\cos\gamma_S)\sum_{i=0}^{2}\sum_{j=-i}^{i}\Psi_{n\ell}(i,j|r)$$

$$G_{Had}(x,x')_{k=0} = \frac{1}{8\pi^2}\sum_{n=-\infty}^{\infty} e^{in\kappa\Delta\tau}\int_0^\infty \alpha J_0(\alpha\gamma_R)\sum_{i=0}^{2}\sum_{j=-i}^{i}\Psi_{n\alpha}(i,j|r)d\alpha$$

$$G_{Had}(x,x')_{k=-1} = \frac{1}{8\pi^2}\sum_{n=-\infty}^{\infty} e^{in\kappa\Delta\tau}\int_0^\infty \rho\tanh(\rho\pi)P_{-\frac{1}{2}+i\rho}(\cosh\gamma_H) \times\sum_{i=0}^{2}\sum_{j=-i}^{i}\Psi_{n\rho}(i,j|r)d\rho$$

The subtraction can then be performed mode-by-mode: the contribution from each mode is manifestly finite.

What should we expect to see?

The value of the vacuum polarisation is constant in a spacetime without a black hole.
In "pure" adS space, this value can be found analytically[4].
If $r_h = 2,\ \Lambda = -3$, then

$$\langle \phi^2 \rangle_{ren} = \frac{-1}{48\pi^2}, \quad \text{Dirichlet bcs}$$

$$\langle \phi^2 \rangle_{ren} = \frac{5}{48\pi^2}, \quad \text{Neumann bcs}$$

[4] C. Kent, E. Winstanley, *Phys. Rev. D*, 2015

Plots of vacuum polarisation[5]

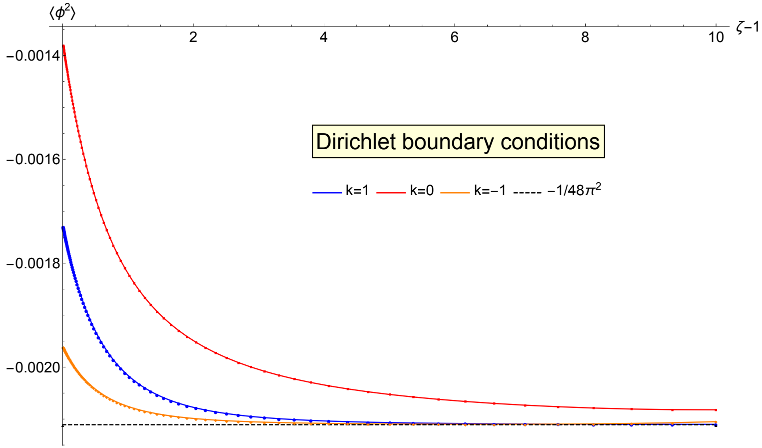

[5] T. Morley, P. Taylor, E. Winstanley, *CQG*, 2018

Plots of vacuum polarisation[5]

*

*

The spacetime

Quantum Field Theory

Vacuum Polarisation

Renormalisation

Plots of vacuum polarisation

Conclusions

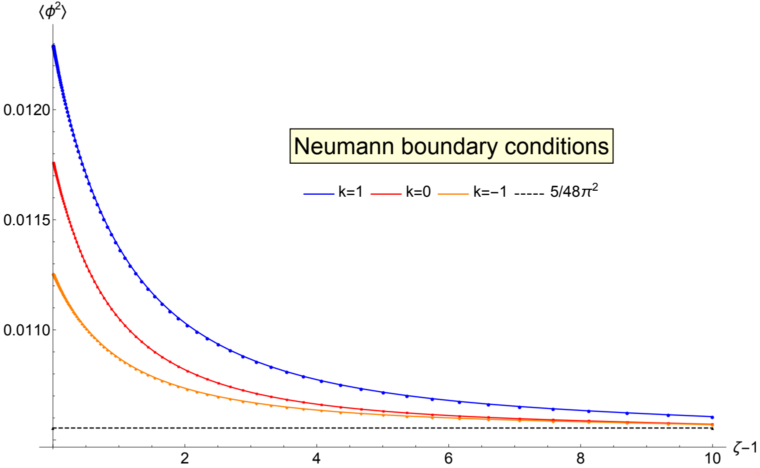

[5] T. Morley, P. Taylor, E. Winstanley, *CQG*, 2018

Conclusions + Outlook

- Despite the same behaviour far from the horizon, $\langle\hat{\phi}^2\rangle_{ren}$ behaves differently close to the horizon for different horizon topologies.

Conclusions + Outlook

- Despite the same behaviour far from the horizon, $\langle\hat{\phi}^2\rangle_{ren}$ behaves differently close to the horizon for different horizon topologies.
- This raises the interesting possibility that the shape of the horizon may be encoded in quantum expectation values.

Conclusions + Outlook

- Despite the same behaviour far from the horizon, $\langle\hat{\phi}^2\rangle_{ren}$ behaves differently close to the horizon for different horizon topologies.
- This raises the interesting possibility that the shape of the horizon may be encoded in quantum expectation values.
- Changing conditions on the boundary affects $\langle\hat{\phi}^2\rangle_{ren}$ on the horizon.

Conclusions + Outlook

- Despite the same behaviour far from the horizon, $\langle\hat{\phi}^2\rangle_{ren}$ behaves differently close to the horizon for different horizon topologies.
- This raises the interesting possibility that the shape of the horizon may be encoded in quantum expectation values.
- Changing conditions on the boundary affects $\langle\hat{\phi}^2\rangle_{ren}$ on the horizon.

Possible future work

Conclusions + Outlook

- Despite the same behaviour far from the horizon, $\langle\hat{\phi}^2\rangle_{ren}$ behaves differently close to the horizon for different horizon topologies.
- This raises the interesting possibility that the shape of the horizon may be encoded in quantum expectation values.
- Changing conditions on the boundary affects $\langle\hat{\phi}^2\rangle_{ren}$ on the horizon.

Possible future work

- Comparison between vacuum states

Conclusions + Outlook

- Despite the same behaviour far from the horizon, $\langle\hat{\phi}^2\rangle_{ren}$ behaves differently close to the horizon for different horizon topologies.
- This raises the interesting possibility that the shape of the horizon may be encoded in quantum expectation values.
- Changing conditions on the boundary affects $\langle\hat{\phi}^2\rangle_{ren}$ on the horizon.

Possible future work

- Comparison between vacuum states
- Compactified event horizons

Conclusions + Outlook

- Despite the same behaviour far from the horizon, $\langle\hat{\phi}^2\rangle_{ren}$ behaves differently close to the horizon for different horizon topologies.
- This raises the interesting possibility that the shape of the horizon may be encoded in quantum expectation values.
- Changing conditions on the boundary affects $\langle\hat{\phi}^2\rangle_{ren}$ on the horizon.

Possible future work

- Comparison between vacuum states
- Compactified event horizons

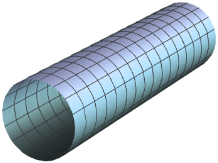

Conclusions + Outlook

- Despite the same behaviour far from the horizon, $\langle\hat{\phi}^2\rangle_{ren}$ behaves differently close to the horizon for different horizon topologies.
- This raises the interesting possibility that the shape of the horizon may be encoded in quantum expectation values.
- Changing conditions on the boundary affects $\langle\hat{\phi}^2\rangle_{ren}$ on the horizon.

Possible future work

- Comparison between vacuum states
- Compactified event horizons

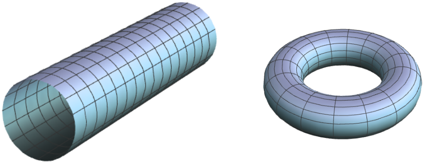

Conclusions + Outlook

- Despite the same behaviour far from the horizon, $\langle\hat{\phi}^2\rangle_{ren}$ behaves differently close to the horizon for different horizon topologies.
- This raises the interesting possibility that the shape of the horizon may be encoded in quantum expectation values.
- Changing conditions on the boundary affects $\langle\hat{\phi}^2\rangle_{ren}$ on the horizon.

Possible future work

- Comparison between vacuum states
- Compactified event horizons